CHIN. PHYS. LETT. Vol. 34, No. 4 (2017) 044301

Distance-Coefficient-Based Imaging Accuracy Improving Method Based on the Lamb Wave

Shao-Jie Chen(陈少杰), Shao-Ping Zhou(周邵萍)**, Yong Li(李勇),
Yan-Xun Xiang(项延训), Min-Xin Qi(戚敏新)

Key Lab of Pressure Systems and Safety (MOE), East China University of Science and Technology, Shanghai 200237

(Received 3 January 2017)

An imaging accuracy improving method is established, within which a distance coefficient including location information between sparse array configuration and the location of defect is proposed to select higher signal-to-noise ratio data from all experimental data and then to use these selected data for elliptical imaging. The relationships among imaging accuracy, distance coefficient and residual direct wave are investigated, and then the residual direct wave is introduced to make the engineering application more convenient. The effectiveness of the proposed method is evaluated experimentally by sparse transducer array of a rectangle, and the results reveal that selecting experimental data of smaller distance coefficient can effectively improve imaging accuracy. Moreover, the direct wave difference increases with the decrease of the distance coefficient, which implies that the imaging accuracy can be effectively improved by using the experimental data of the larger direct wave difference.

PACS: 43.60.Lq, 43.35.Cg, 43.20.Mv DOI: 10.1088/0256-307X/34/4/044301

The Lamb wave has attracted considerable attention for structural health monitoring (SHM) of plate-like structure because of its capability of propagating along the plane of plate-like structures with slight propagation loss and sensitivity to both surface and subsurface features.[1–3] The imaging algorithm is critical for damage localization by using the Lamb wave method, and in the past few years, it has been widely investigated by many researchers. Michaels *et al.*[4] proposed an ellipse damage localization algorithm based on the TDOA model. Yu *et al.*[5] developed an imaging algorithm of focusing array for Lamb wave. After that, a baseline-free inspection method for composite plates using a virtual time reversal imaging algorithm was developed by Jeong *et al.*[6] De *et al.*[7] proposed a defect localization method by the combination of the probability ellipse and artificial neural networks. The technology of baseline subtraction plays a key role in many imaging algorithms. However, the residual signal is strongly impacted by noise, dispersion, multi-mode characteristic of the guided wave and reflection from structural boundaries, which seriously degrade imaging accuracy. To resolve these problems, several methods are studied from different fields. Hayashi *et al.*[8] employed the FFT transform to realize the separation of A0 and S0 modes. Crazy climber algorithm was used by Xu *et al.*[9] to deal with multi-mode signal. A method of dispersion compensation is proposed by Xu *et al.*[10] to realize the separation of A0 and S0 mode. Park *et al.*[11] used the group velocity ratio rule and the mode amplitude ratio rule to achieve mode decomposition of the Lamb wave. The combination of the MVDR method and the two-dimensional array is studied by Engholm *et al.*[12] to reduce the influence of interfering Lamb wave modes. The influence of various internal and external noises on imaging performance is inevitable. When Lamb waves are propagating in plate-like structures, the signals are always interfered with by noise,[13] which always has a significant influence on extraction of the scattering signal from the time-domain signal. Continuous wavelet transform was employed by Liu *et al.*[14] to remove noise. Michaels *et al.*[15] used digital band-pass filtering to reduce complexity of the signals, and then defects were detected and localized by using a signal after the filter.

Although the aforementioned studies have shown different levels of success in improving imaging accuracy, in practice, the residual data obtained by baseline subtraction often contain some lower signal-to-noise ratio (SNR) data, which may have a significant influence on imaging accuracy. Therefore, how to select higher SNR data from all residual data is still a challenge for improvement of imaging accuracy. The main innovation of this study is to provide a method of how to choose higher SNR (signal-to-noise ratio) data from all test data and then to use these selected data for elliptical imaging. Compared with current technologies such as probability damage algorithm, time reversal algorithm, the method has both the advantages of improving the defect location accuracy and easy to implement.

To detect defects of plate-like structure using the Lamb wave, the fundamental theory of imaging algorithm is briefly introduced. As shown in Fig. 1(a), the incentive sensor T and receiving sensor R are attached in the plate, where the point D is the location of the defect. The Lamb wave generated by the sensor T

**Corresponding author. Email: shpzhou@ecust.edu.cn

propagates to the location of defect D, and then is scattered by the defect D; finally the scattering signal is received by the receiving sensor R. The time of scattering signal t is considered directly from a time domain waveform. In addition, the group velocity of the Lamb wave $v_{\rm g}$ can be read directly from the dispersion curve.

The propagation distance $d_{\rm T-D-R}$ of S_0 modes can be calculated by

$$d_{\rm T-D-R} = d_{\rm TD} + d_{\rm RD} = v_{\rm g} t. \tag{1}$$

The S_0 mode is excited at point T (PZT T), propagates to the defect D and then is reflected by D. The reflected signal is received by point R (PZT R).

According to the geometric relations of the ellipse, it can be seen that defect D is on the elliptical trajectory where sensors T and R are the focuses and $d_{\rm T-D-R}$ is the long axis (as shown in Figs. 1(a) and 1(b)), which is the principle of the ellipse location of the defect.

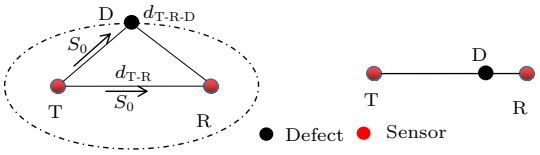

Fig. 1. Ellipse imaging algorithm: (a) defect is not in the direct path, and (b) defect is in the direct path.

Consider a sensor pair ij, where the ith transducer (the transmitter) is located at (x_i, y_i), and the jth transducer (the receiver) is located at (x_j, y_j). The time, taking account of when the Lamb wave is generated by the incentive sensor (x_i, y_i), propagated to any discrete point (x, y) of the plate, and then reflected to the receiving sensor (x_j, y_j), is determined by

$$t_{xy}^{ij} = [\sqrt{(x_i - x)^2 + (y_i - y)^2} + \sqrt{(x_j - x)^2 + (y_j - y)^2}]/v_{\rm g}. \tag{2}$$

Let $s_{ij}(t)$ refer to the amplitude of the difference signal computed by baseline subtraction for the sensor pair ij, the defect imaging results $I_{xy}(t)$ can be calculated by

$$I_{xy}(t) = \prod_{i=1}^{N} \prod_{j=1, j\neq i}^{N} s_{ij}(t_{xy}^{ij}), \tag{3}$$

where N is the number of sensors of sparse array. Ideally, by subtracting baseline signals recorded from the damage-free structure from current test signals, a residual signal assumed to arise from damage is obtained. These residual signals can be applied to ellipse imaging for damage detection and localization. However, the ellipse imaging algorithm is strongly affected by a mismatched environment and operational condition. Therefore, the reflection signal resulting from the boundary and noise cannot be completely eliminated by baseline subtraction. In addition, the single-mode (such as the S_0 mode) will be converted into all possible modes (such as $S_0 + A_0 + SH_0$) when the Lamb wave interacts with the defect, and the Lamb wave of the conversion (such as $A_0 + SH_0$) cannot be eliminated by the baseline subtraction. These factors will seriously reduce the signal-to-noise ratio (SNR) of some residual signals, and affect the imaging accuracy. Therefore, the residual signal with a higher SNR can improve the imaging accuracy.

Imaging performance for structural health monitoring using the Lamb wave is often impacted by the number of sensors, array diameter and location of defect. Hall *et al.*[16] investigated that the signal-to-noise ratio increases with the number of transducers. Wandowski *et al.*[17] indicated that the directivity of imaging result correlates with distance between transducers (array diameter). Although the aforementioned investigations have shown that the imaging accuracy is closely related to the location of defects relative to incentive and receiving sensor, how to qualitatively study this relationship is still unclear. Therefore, the distance coefficient is defined in this work to study the relationship between imaging accuracy and location of defect relative to the sensor pair ij including excitation and receiving sensors. The distance coefficient η is given by

$$\eta = \frac{d_{\rm TD} + d_{\rm RD}}{d_{\rm TR}}, \tag{4}$$

where $d_{\rm TD}$ is the distance between the incentive sensor T and defects D, $d_{\rm RD}$ is the distance between the receiving sensor R and defects D, and $d_{\rm TR}$ is the distance between the incentive sensor T and receiving sensor R.

Equation (4) shows the positional relationship among the incentive sensor, the receiving sensor and the defect. As shown in the formula, the distance coefficient is not less than 1, and the distance coefficient can be determined by both locations of the defects and the sensor pair ij where the ith is used as exciting and the jth is used as receiving. When the defect location or the sensor pair ij changes, the distance coefficient also changes. Moreover, the smaller the distance coefficient is, the closer the defect is to the line between the sensor pair ij (ith as exciting and jth as receiving), and this indicates that the scattering signal would be superimposed with the direct wave signal (Lamb waves transmitted directly from the excitation sensor to the receiving sensor or the first wave packet in the time domain signal recorded by receiving sensor) at this moment because of extremely fast speed of propagation of the Lamb wave. In addition, when the distance coefficient is 1, defect D is located between excitation and receiving sensors (as shown Fig. 1(b)),

which indicates that the direct wave recorded by the receiving sensor R is a transmission wave (or forward-scattered wave). Figure 2 shows the energy distribution of the S_0 mode interacting with through-hold defect in the plate. As shown in Fig. 2, mode converse and scattering would be generated when the incident wave interacts with the hole defect. However, the energy distribution of the scattering wave around the defect is extremely unbalanced. From Fig. 2, it can be seen that forward-scattered waves of the S_0 mode (distance coefficient $\eta = 1$ or η close to 1) are significantly larger in amplitude than the other direction scattered wave (distance coefficient $\eta \gg 1$), and other Lamb wave modes are generated due to mode converse. Therefore, the test data with smaller distance coefficient can obtain a larger scattering signal, which improves the imaging accuracy.

Since the location of defect is unknown in the actual monitoring, the distance coefficient cannot be computed directly even if the array diameter has been determined. As discussed above, however, the scattering signal would be superimposed with the direct wave signal when the distance coefficient is at a smaller value, which leads to a significant change in the direct wave compared with the damage-free structure. With the increase of the distance coefficient, the scattered signal gradually separates from the direct wave packet, which means a decreasing change in the direct wave. Therefore, the range of the distance coefficient can be determined by the residual direct wave.

Direct wave refers to the first wave packet in time-domain signal. In this study, the residual direct wave signal is obtained by subtracting baseline direct signals recorded from the damage-free structure from the current direct signal. The Hilbert transform is performed for the residual direct wave signal to obtain the envelope of the signal. However, the envelope of the residual direct wave contains hundreds of amplitude points. Therefore, the maximum value of the envelope signal is selected as an indicator of the residual direct wave to explore the relationship between the distance coefficient and the residual direct wave signal. The Hilbert transformation of residual direct wave and the maximum value of the envelope signal are given by

$$H(\Delta u_{ij})(t) = \frac{1}{\pi} \int_{-\infty}^{\infty} \frac{\Delta u_{ij}(\tau)}{t - \tau} d\tau, \tag{5}$$

$$s_{ij} = \max(||H(\Delta u_{ij})(k)||), \tag{6}$$

where t is the time in the wave packet of the residual direct wave signal, Δu_{ij} is the residual direct wave obtained from baseline subtraction and ij is the number of a pair of sensors including excitation and receiving sensors. As described above, the scattering signal would be superimposed completely with the direct wave signal when the distance coefficient is 1.0, and with the increase of the distance coefficient, the scattering signal is gradually separated from the direct wave, where the residual direct wave signal decreases with the increase of the distance coefficient. Therefore, there is a definite relationship between the distance coefficient and the residual direct wave signal.

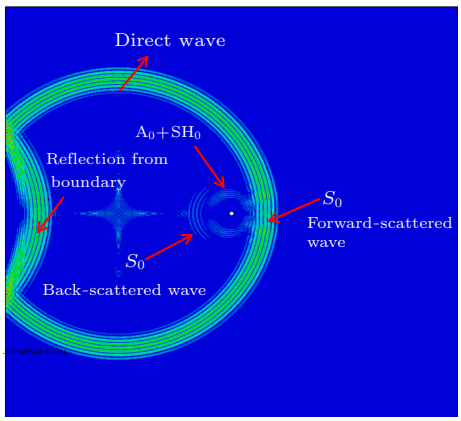

Fig. 2. Scattered field distribution.

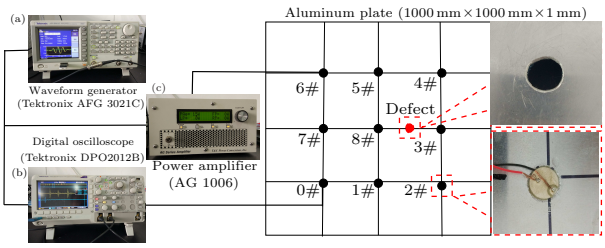

Fig. 3. Experimental setups of (a) waveform generator, (b) digital oscilloscope and (c) signal amplifier.

Experiments are performed on an aluminum plate with the length of 1000 mm, width of 1000 mm, thickness of 1 mm, and the sparse transducers array of a rectangle is introduced for defects localization. Defects of through-hole with diameter of 10 mm are made in the aluminum plate. Figure 3 shows the experimental setup. The experimental system includes a waveform generator (Tektronix AFG 3021C), a power amplifier (AG 1006), a digital oscilloscope (Tektronix DPO2012B), a changeover switch, a computer, and sparse array of piezoelectric transducers with size of 10 mm (diameter) ×1 mm (thickness) in which the distance between the adjacent sensors is 200 mm.

The selection of excitation mode and frequency range is very important for the use of ultrasonic guided waves inspection. Dispersion curves are the essential tool to optimize mode and frequency. Figure 4(a) shows the dispersion curves of phase and group velocity of the aluminum plate (the length of 1000 mm, width of 1000 mm, and thickness of 1 mm). According to the dispersion curves in Fig. 4(a), ranging from 80 kHz to 500 kHz, only two basic modes of S_0 and A_0 are shown and the dispersion has slight influence on the mode of S_0 and has a larger influence on the

mode of A_0 in these frequency. Figure 4(b) shows the amplitude of modes of S_0 and A_0 processed by normalization from 80 kHz to 500 KHZ. As shown in Fig. 4(b), the amplitude of S_0 mode is much greater than that of A_0 at 300 kHz. Consequently, the 300 kHz frequency is chosen as excitation frequency to reduce the effects of both dispersion and multi-mode on the experiment.

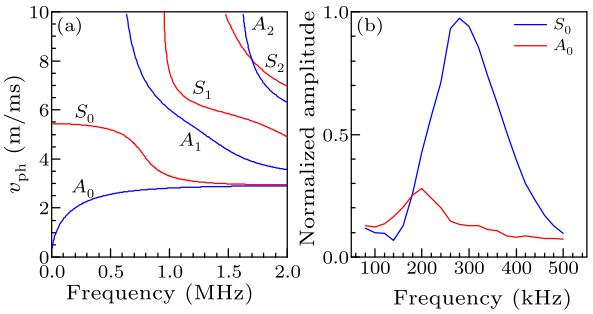

Fig. 4. (a) Dispersion curves of the Lamb wave. (b) Amplitude of A_0 and S_0 modes.

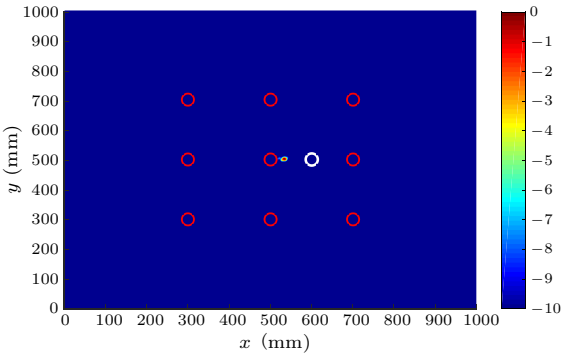

Fig. 5. Imaging using all the experimental data.

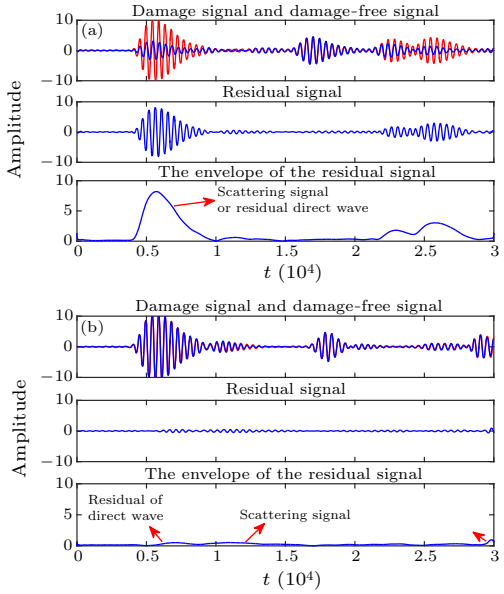

Fig. 6. Time-domain wave: (a) for the distance coefficient 1.0, and (b) for the distance coefficient 2.0.

To inspect and localize defects including crack and hole-through, the imaging algorithm is used in structural health monitoring of plate-like structures. Figure 5 shows the imaging result using all test signals. As shown in Fig. 5, the result is very different from the actual location of the defect, due to the fact that a large number of test data contain some lower SNR signal because of the noise and reflection from boundary. The distance coefficient has been defined to explore the relationship between the distance coefficient and SNR of text data. Figure 6 shows the two time-domain waves including the original signal measured by experiment, the residual signal computed by baseline subtraction and the envelope of the residual signal obtained by the Hilbert transform, where the distance coefficients (computed by Eq. (4)) are at 1.0 and 2.0, respectively. From Fig. 6, it can be seen that there are higher SNR of residual signals when the distance coefficient is at 1.0. However, with the increase of the distance coefficient, noise and reflection from the boundary have increasing influence on the residual signal, which results in decreasing signal-to-noise ratio of the residual signal. Therefore the residual signal obtained by the sensor pair ij with a smaller distance coefficient has a larger signal-to-noise ratio, which indicates that the imaging accuracy can be improved by selecting residual data with a smaller distance coefficient.

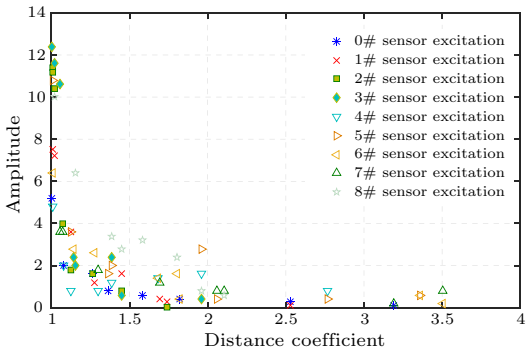

Fig. 7. The distance coefficient and the residual direct wave.

As described above, the residual direct wave signal (computed by Eqs. (5) and (6)) decreases with the increase of the value distance coefficient. Figure 7 shows that the residual direct wave varies with the increase of the distance coefficient in the square sparse array. As shown in Fig. 7, the amplitude of the residual direct wave decreases with the increase of the distance coefficient. Moreover, the amplitude of the residual direct wave sharply decreases with the increase of the distance coefficient when the value of distance coefficient is in the range of 1–1.3, and then it gradually tends to zero when the value of distance coefficient is higher than 1.3. As discussed above, the amplitude of the residual direct wave decreases with the increase of the distance coefficient. Combined with the above theory, of which the residual signal with smaller dis-

tance coefficient has a larger signal-to-noise ratio, it can be seen that the residual signal with larger value of residual direct wave has a larger signal-to-noise ratio, which indicates that the imaging accuracy is improved by selecting residual data with a larger value of the residual direct wave.

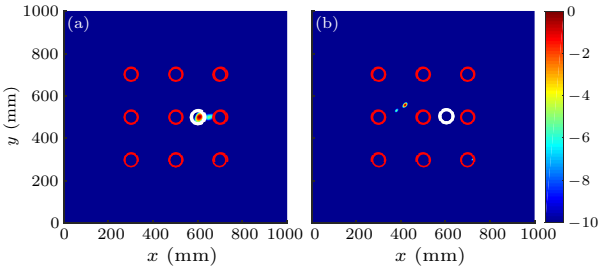

Fig. 8. Imaging result: (a) the distance coefficient is in the range of 1–1.5, and (b) the distance coefficient is larger than 1.5.

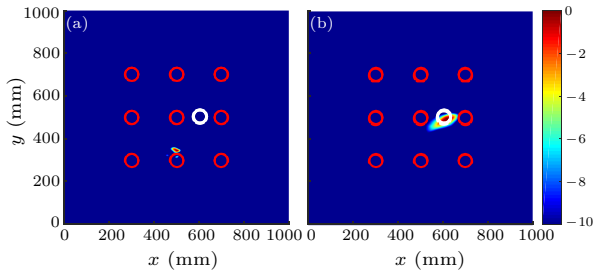

Fig. 9. Imaging result: (a) the residual direct wave is in the range of 0–1, and (b) the residual direct wave is larger than 3.

As discussed above, it is effective to improve the imaging accuracy by selecting the experimental data with a smaller distance coefficient. Figure 8 shows that the imaging algorithm is performed by selecting experimental data with different distance coefficients in sparse transducer array of rectangle. Figures 8(a) and 8(b) show that the imaging algorithm is performed by the experimental data with distance coefficients from 1 to 1.5, and higher than 1.5, respectively. Figure 8(a) shows that the image constructed by selecting residual signal with the distance coefficient of 1–1.5 is coincident with the location of the actual defect. Compared with Fig. 5, its imaging accuracy is obviously improved in Fig. 8(a). From Fig. 8(b), it can be seen that the image constructed by selecting the residual signal with the distance coefficient of higher than 1.5 is very different from the actual location of the defect. Compared with Fig. 5, its imaging accuracy in Fig. 8(b) is obviously degraded. According to the above discussion, the imaging accuracy can be improved by selecting residual data with a smaller value of distance coefficient.

Figure 9 shows four images that were constructed by selecting data with residual direct wave of 0–1 and higher than 3, respectively. Figure 9(a) demonstrates that the image constructed by selecting the residual signal with residual direct waves of 0–1 is very different from the location of the actual defect. Figure 9(b) shows the image that is generated by selecting the residual signal with residual direct wave of higher than 3. As shown in Fig. 9(b), the imaging results are completely coincident with the location of the actual defect. Compared with Fig. 5, it can be seen that the imaging accuracy can be effectively improved when the imaging algorithm is performed by selecting residual data with a larger deference value of the direct wave.

In summary, a distance coefficient-based imaging accuracy improving method has been proposed. One finding is that the residual signal obtained by the sensor pair ij with a smaller distance coefficient has a larger signal-to-noise ratio, which indicates that the imaging accuracy can be improved by selecting residual data with a smaller distance coefficient. The other finding is that the value of the residual direct wave decreases with the increase of the distance coefficient. Therefore, in the process of defect detection and location using baseline subtraction, imaging accuracy can be effectively improved by selecting residual data with a larger value of residual direct wave to perform the imaging algorithm in the plate-like structure.

References

[1] Zhang H Y, Ruan M, Zhu W F and Chai X D 2016 *Chin. Phys.* B **25** 124304
[2] Li M L, Deng M X and Gao G J 2016 *Chin. Phys.* B **25** 124301
[3] Zhang H Y, Chen X H, Cao Y P and Yu J B 2010 *Chin. Phys. Lett.* **27** 104301
[4] Michaels J E 2008 *Smart Mater. Struct.* **17** 035035
[5] Yu L and Leckey C A C 2012 *J. Intel. Mat. Syst. Struct.* **22** 1138
[6] Jeong H, Cho S and Wei W 2011 *Chin. Phys. Lett.* **28** 064301
[7] De Fenza A, Sorrentino A and Vitiello P 2015 *Compos. Struct.* **133** 390
[8] Hayashi T and Kawashima K 2003 *JSME Int. J. A-Mech. Mater. Eng.* **46** 620
[9] Xu K, Ta D and Wang W 2010 *IEEE Trans. Ultrason. Ferroelectr. Freq. Control* **57** 2480
[10] Xu K, Ta D and Moilanen P 2012 *J. Acoust. Soc. Amer.* **131** 2714
[11] Park I, Jun Y and Lee U 2014 *Wave Motion* **51** 335
[12] Engholm M and Stepinski T 2010 *IEEE Trans. Ultrason. Ferroelectr. Freq. Control* **57** 2712
[13] Niri E D, Farhidzadeh A and Salamone S 2013 *Struct. Health Monit.* **12** 59
[14] Liu Z, Sun K and Song G 2016 *Mech. Syst. Signal Process.* **70** 625
[15] Michaels J E and Michaels T E 2007 *Wave Motion* **44** 482
[16] Hall J S and Michaels J E 2011 *37th Annu. Rev. Prog. Quant. Nondestructive Eval. (QNDE)* (San Diego USA, 18–23 July 2010) p 859
[17] Wandowski T, Malinowski P H and Ostachowicz W M 2016 *Mech. Syst. Signal Process.* **66** 248